

van der Waals Interactions of Parallel and Concentric Nanotubes

Elsebeth Schröder and Per Hyldgaard*

*Department of Applied Physics, Chalmers University of Technology
and Göteborg University, SE-412 96 Gothenburg, Sweden*

(Dated: June 11, 2003)

For sparse materials like graphitic systems and carbon nanotubes the standard density functional theory (DFT) faces significant problems because it cannot accurately describe the van der Waals interactions that are essential to the carbon-nanostructure materials behavior. While standard implementations of DFT can describe the strong chemical binding within an isolated, single-walled carbon nanotube, a new and extended DFT implementation is needed to describe the binding between nanotubes. We here provide the first steps to such an extension for parallel and concentric nanotubes through an electron-density based description of the materials coupling to the electrodynamic field. We thus find a consistent description of the (fully screened) van der Waals interactions that bind the nanotubes across the low-electron-density voids between the nanotubes, in bundles and as multiwalled tubes.

I. INTRODUCTION

Soft and sparse materials constitute an important challenge for our first-principle quantum-physical account of structure and dynamics. These structures are defined by voids of very-low-electron density regions across which material binding is communicated exclusively via the coupling to the electrodynamic fields, the so-called dispersion or van der Waals (vdW) forces. Traditional implementations of density functional theory (DFT) cannot account for this type of interaction because the density functionals (DF) are defined as local or semilocal and fail to describe the truly nonlocal nature of the electrodynamic coupling. Nevertheless, the traditional approaches are imperative for accurate predictions of the binding within the dense regions of finite electron densities. The many opportunities in biological systems, in organic-molecular liquids and in the carbon nanostructures motivate a continuous search for a consistent combination of traditional DFT and vdW corrections. This biophysics and nanotechnology perspective motivated our recent proposal for a vdW-DF for layered systems [1, 2, 3, 4].

The interaction in nanotube bundles, ropes [5], and within multiwalled nanotubes [6], as addressed here, represents another type of sparse-matter problem with a nanotechnological relevance [7]. Nanotube bundles are often directly produced and/or extracted to align the nanotube for Raman spectroscopy whereas multiwalled nanotubes are produced in many fabrication techniques. Both the nanotube bundles and the concentric multiwalled nanotubes are stabilized by a competition between the kinetic-energy repulsion and the long-ranged van der Waals binding. At the relevant binding distances (3 to 3.5 Å or 6 to 7 Bohr radii) the traditional first-principle DFT calculations cannot account for the combined interaction. The issues and challenges are similar to and closely related to the corresponding problem of ab-initio calculations of the binding in graphite [4].

An accurate quantum-physics account of the binding in nanotube bundles and in multiwalled nanotubes must include a calculation of the dispersion forces defined by the electrodynamic coupling. To illustrate the importance of these van der Waals contributions we here use a simple model description of the single-tube electrodynamic response fitted to DFT calculation of the nanotube electron system and response. While simple, our approach improves the traditional Hamaker-type of estimates [8] in several ways: (i) it offers a method for a first-principle calculation of the interaction strength, (ii) it includes the important local-field screening effects as directly defined by the anisotropic spatial variation in the nanotube electron density (which we here obtain from DFT); and (iii) it consistently accounts for the net anisotropic dielectric response that describes extended molecules. In this manner we establish a link between the microscopic description (based on accurate

*E-mail: hyldgaard@fy.chalmers.se

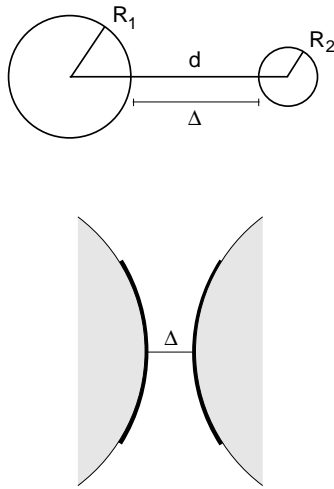


FIG. 1: Sketch of parallel nanotubes. *Top panel:* Tubes with radii R_1 and R_2 , seen along the z_1 and z_2 axes. *Bottom panel:* A closer look at the closest interaction region. Whereas all parts of a nanotube in principle interact with all parts of the other nanotube the strongly attractive character of the dipole-dipole interaction causes most of the contribution to the collective interaction to come from within the region near the line of closest contact.

DFT calculations of the electron density variations and static susceptibility [4]) and the phenomenologic descriptions, and we provide a method to test the limit of applicability. In a wider sense our nanotube study also provides an indirect insight on how the electron-density variation determines the optical response of large extended (organic) molecules as used, for example, in liquid-crystal displays [9].

In the present analysis of the nanotube van der Waals interaction we focus on interaction strength at intermediate separations when the interaction is defined by the dipolar contribution [4, 10]. This emphasis permits a number of very important simplifications. With a set of approximations we succeed in using the high degree of symmetry which exists in the case of parallel and concentric nanotubes to split the interaction into an effective coupling constant (given by one frequency integration) and a nanotube geometry factor. In the worst case the computation is thus reduced to just a two-dimensional spatial integration, as shown in the following. Moreover, both for the cases of concentric nanotubes and of identical parallel nanotubes we further succeed in expressing this general integral fully or partially in terms of spatial function for additional efficiency gain.

II. THE NANOTUBE ELECTRODYNAMIC RESPONSE

Our calculations of the physical intertube attraction are based on accurate first-principle DFT calculations of the nanotube electron density, the overall, nanotube electrostatic response, and an approximate treatment of the nanotube electrodynamical response, local-field effects, and resulting intertube attraction. The approach is described in Ref. [11] and will be summarized here.

Adapting the plasmon-pole model of Ref. [10], we approximate the local microscopic electron response (for a sub-atomic-scale element of the nanotube wall) by the bare dynamic susceptibility $\chi_0(n(\mathbf{r}), u, u_0) = n(\mathbf{r})/(u^2 + u_0^2)$ at (complex) frequency u . Hartree atomic units are used with symbols a_0 for the Bohr radius and Ha for the hartree (≈ 27.21 eV). The nanotube electron density $n(\mathbf{r})$ (at position \mathbf{r}) is determined directly from first-principle DFT calculations, and the value of the effective frequency cut-off u_0 is obtained by comparing first-principle calculations of the static nanotube susceptibility to a calculation including the local-field effects produced by the model of χ_0 .

From this model of χ_0 we obtain a corresponding effective susceptibility tensor χ_{eff} which describes the ratio of the locally induced polarization to the externally applied electric field. We describe the response of a nanotube to an applied electric field using a local cylindrical coordinate

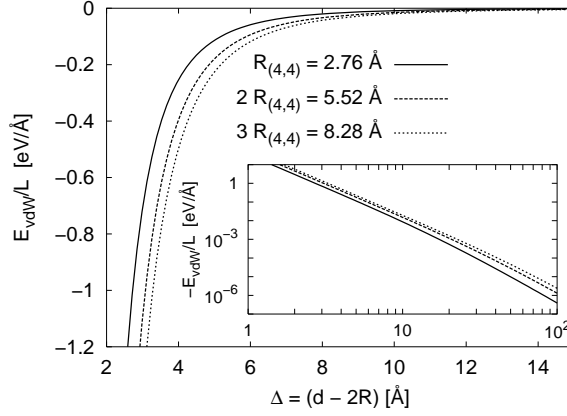


FIG. 2: Van der Waals interaction of pairs of parallel nanotubes with pairwise identical radii, as a function of smallest separation $\Delta = d - 2R$. The attraction of large nanotubes (radius $3R_{(4,4)}$) is greater than that of small tubes (radius $R_{(4,4)}$) at the same Δ . Large nanotubes have less curvature and thus at a given distance Δ a pair of large tubes has a larger amount of charge at distance approximately Δ , yielding a larger total binding per tube length.

system (s, θ, z) with the z -axis along the nanotube axis and \mathbf{s} a vector perpendicular to the z -axis. Approximating the nanotube electron density $n(\mathbf{r})$ by its radially averaged value $n(s)$ the local effective susceptibility is given by the relation

$$\chi_{\text{eff}}[n(s)](u)\mathbf{E}_{\text{applied}} = -\chi_0(n(s), u, u_0)\nabla\phi(\mathbf{s}, u) \quad (1)$$

where the local electric field $-\nabla\phi(\mathbf{s}, u)$ is given by charge conservation $\nabla \cdot \{(1 + 4\pi\chi_0)\nabla\phi\} = 0$. In general, the effective susceptibility tensor χ_{eff} will be anisotropic with off-diagonal elements. However, when transforming the tensor χ_{eff} into cylindrical coordinates all off-diagonal elements vanish and only the diagonal elements $\hat{\chi}_{\text{eff}}^\beta$, $\beta = s, \theta, z$ are left.

For an external electric field of strength $E_0(u)$, oriented perpendicular to the nanotubes or along the nanotubes, we may factorize the electric potential as $\phi(\mathbf{s}, u, u_0) = -E_0(u)W(s, u, u_0)\cos\theta$ and solve $\nabla \cdot \{(1 + 4\pi\chi_0)\nabla\phi\} = 0$. The components of the effective susceptibility then become [11] $\hat{\chi}_{\text{eff}}^s = \chi_0\partial_s W$, $\hat{\chi}_{\text{eff}}^\theta = \chi_0 W/s$, and $\hat{\chi}_{\text{eff}}^z = \chi_0$.

To proceed with an efficient determination of the internanotube van der Waals interactions we exploit the special form of the nanotube electron density. In the thin-wall approximation we approximate the radial behavior of the effective susceptibility $\hat{\chi}_{\text{eff}}^\gamma(s, u, u_0) \rightarrow \tilde{\chi}^\gamma(R, u, u_0)\delta(s - R)$, by a weighted radial delta function such that $\int d^2s \hat{\chi}_{\text{eff}}^\gamma(s, u, u_0) \equiv 2\pi R \tilde{\chi}^\gamma(R, u, u_0)$.

These approximations are the basis for derivation of the nanotube-nanotube interaction.

III. THE NANOTUBE-NANOTUBE VAN DER WAALS INTERACTION

For a pair of parallel nanotubes at center-to-center separation d (Fig. 1) we define two sets of local cylindrical coordinate systems with origos separated by d , and with indices 1 and 2 referring to the two nanotubes and their local coordinate systems. Within the dipole-dipole approximation we then find the van der Waals energy

$$E_{\text{vdW}} = -\frac{1}{2\pi} \int_0^\infty du \text{Trace} \{ \hat{\chi}_1 T_{12}(d) \hat{\chi}_2 T_{21}(d) \} \quad (2)$$

$$= -\frac{L}{2\pi} \sum_{\beta, \gamma = s, \theta, z} \left(\int_0^\infty du \tilde{\chi}^\beta(R_1, u, u_0^{(1)}) \tilde{\chi}^\gamma(R_2, u, u_0^{(2)}) R_1 R_2 \right) \times \int_0^{2\pi} d\theta_1 \int_0^{2\pi} d\theta_2 I_{\beta\gamma}(\theta_1, \theta_2, R_1, R_2) \quad (3)$$

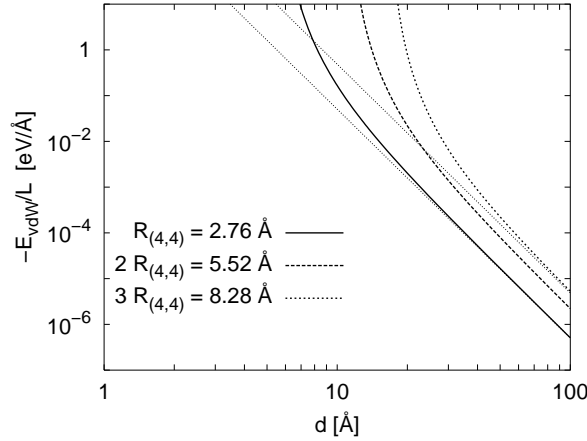


FIG. 3: Van der Waals interaction of pairs of parallel nanotubes as a function of center-of-tube to center-of-tube distance d . Gray lines are the asymptotes $E_{\text{vdW}}/L \sim -C_5/d^5$ with $C_5 = 9\pi^2 J_{\text{tot}}(R, R, u_0, u_0)/64$ for $R = R_{(4,4)}$ and $R = 3R_{(4,4)}$.

with the geometry terms

$$\begin{aligned}
 I_{\beta\gamma}(\theta_1, \theta_2, s_1, s_2) &= \frac{1}{L} \int_{-L/2}^{L/2} dz_1 \int_{-\infty}^{\infty} dz_{21} T_{12}^{\beta\gamma}(d) T_{21}^{\gamma\beta}(d) \\
 &= \int_{-\infty}^{\infty} dz_{21} \left(T_{12}^{\beta\gamma}(d) \right)^2
 \end{aligned} \tag{4}$$

and the dipole coupling $T_{12} = -\nabla_1 \nabla_2 |\mathbf{r}_2 - \mathbf{r}_1|^{-1}$ between elements of the two nanotubes. We made use of the thin-wall approximations to carry out the s_1 and s_2 integrations. The geometry terms $I_{\beta\gamma}$ are of a form for which the z_{21} integration can be easily be carried out [12, (3.241.4)]:

$$\int_{-\infty}^{\infty} dz_{21} \frac{z_{21}^{\mu-1}}{(s_{21}^2 + z_{21}^2)^5} = \frac{\Gamma(\frac{\mu}{2}) \Gamma(5 - \frac{\mu}{2})}{24} s_{21}^{-(10-\mu)} \tag{5}$$

with $\mu = 1, 3, \text{ or } 5$, and $s_{21} = |\mathbf{s}_2 - \mathbf{s}_1|$.

The cut-off frequencies $u_0^{(1)}$ and $u_0^{(2)}$ for the two nanotubes depend in principle on the nanotube radius, but as found in Ref. [11] the macroscopic susceptibility is not very sensitive to the value u_0 . In practice we thus take the large-nanotube value of u_0 for all nanotubes, $u_0^{(1)} = u_0^{(2)} = 0.30 \text{ Ha}$.

For parallel nanotubes we can thus reduce the original simultaneous six-dimensional spatial ($\mathbf{r}_1, \mathbf{r}_2$) and one-dimensional (u) frequency integral to a sum of terms each factorized into a one-dimensional frequency integral times a two-dimensional (θ_1, θ_2) spatial integral. The frequency integrals, now decoupled from the spatial integrals, do not depend on the nanotube separation d and are therefore identical to the frequency factors defined in Ref. [11]

$$J_{\beta\gamma}(R_1, R_2, u_0^{(1)}, u_0^{(2)}) = \int_0^{\infty} du \tilde{\chi}^{\beta}(R_1, u, u_0^{(1)}) \tilde{\chi}^{\gamma}(R_2, u, u_0^{(2)}) R_1 R_2 . \tag{6}$$

As shown earlier [11], the special case of concentric nanotubes ($d = 0$) further reduces the number of spatial dimensions to be integrated.

In general it is not possible to carry out all of the nine spatial integrals $I_{\beta\gamma}(\theta_1, \theta_2, s_1, s_2)$ to express them in terms of known functions. The complications, however, are reduced for certain special cases such as concentric nanotubes [11] and, as shown below, for parallel nanotubes of equal radius.

To emphasize the effect of the cylindrical symmetry on the van der Waals interaction (3) we would like to pursue analytic calculations as far as possible. For this reason we shall assume that the effective radial and tangential susceptibility are identical, $\tilde{\chi}^s \equiv \tilde{\chi}^{\theta}$. The error of this approximation

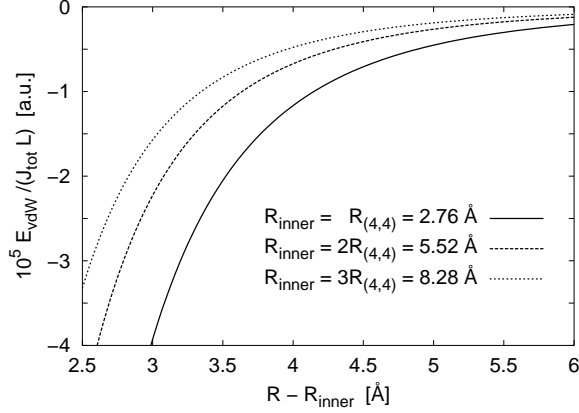


FIG. 4: The geometry part of the van der Waals interaction of concentric nanotubes for fixed inner-tube radius R_{inner} and as a function of outer-tube radius R .

is largest for small frequencies u , and is at most 10%. Thus, with $J_{ss} = J_{\theta s} = J_{s\theta} = J_{\theta\theta}$, $J_{sz} = J_{\theta z}$, and $J_{zs} = J_{z\theta}$, the van der Waals energy per nanotube length becomes

$$\frac{E_{\text{vdW}}}{L} = -\frac{1}{2\pi} \int_0^{2\pi} d\theta_1 \int_0^{2\pi} d\theta_2 \{ J_{ss} (I_{ss} + I_{s\theta} + I_{\theta s} + I_{\theta\theta}) + J_{sz} (I_{sz} + I_{\theta z}) + J_{zs} (I_{zs} + I_{z\theta}) + J_{zz} I_{zz} \}. \quad (7)$$

In Eq. (7) each sum of I -terms has the same functional form,

$$I_{\text{tot}}(\theta_1, \theta_2, R_1, R_2) = \frac{9\pi}{128} ((R_2 \cos \theta_2 + d - R_1 \cos \theta_1)^2 + (R_2 \sin \theta_2 - R_1 \sin \theta_1)^2)^{-5/2} \quad (8)$$

times an integer factor: $I_{ss} + I_{s\theta} + I_{\theta s} + I_{\theta\theta} = 3I_{\text{tot}}$, $I_{sz} + I_{\theta z} = 5I_{\text{tot}}$, $I_{zs} + I_{z\theta} = 5I_{\text{tot}}$, $I_{zz} = 19I_{\text{tot}}$. This is an important observation, as it enables the factorization into frequency and spatial integrals not only for each term in the sum of (7), but indeed for the full sum of (7). If we therefore define an effective frequency integral $J_{\text{tot}} = 3J_{zz} + 5J_{zs} + 5J_{sz} + 19J_{ss}$ the van der Waals energy per length can be written as the product

$$\frac{E_{\text{vdW}}}{L} = -\frac{1}{2\pi} J_{\text{tot}}(R_1, R_2, u_0^{(1)}, u_0^{(2)}) \int_0^{2\pi} d\theta_1 \int_0^{2\pi} d\theta_2 I_{\text{tot}}(\theta_1, \theta_2, R_1, R_2) \quad (9)$$

Eq. (9) is our result for arbitrary-size parallel nanotubes, including concentric nanotubes. The two- and one-dimensional spatial and frequency integrals involved in (9) are already a considerable simplification compared to the original 6 + 1 dimensional integral, and can be numerically solved.

For identical nanotubes, $R_1 = R_2 = R$, the two spatial integrals in (9) further reduce to a single integral over the variable $\xi = (\theta_2 - \theta_1)/2$

$$\begin{aligned} \frac{E_{\text{vdW}}}{L} &= -\frac{9\pi}{64} J_{\text{tot}}(R, R, u_0, u_0) \times \\ &\times \int_{-\pi/2}^{\pi/2} d\xi {}_2F_1 \left(\frac{5}{4}, \frac{7}{4}; 1; \left(\frac{4dR \sin \xi}{d^2 + 4R^2 \sin^2 \xi} \right)^2 \right) (d^2 + 4R^2 \sin^2 \xi)^{-5/2} \end{aligned} \quad (10)$$

where ${}_2F_1$ is a hypergeometric function. Replacing one integral in this way with a well-known, tabulated special function speeds up the numerical evaluation of E_{vdW} and enhances the accuracy.

In Figure 2 we plot E_{vdW} as a function of the smallest distance between elements of the nanotubes, $\Delta = d - R_1 - R_2 = d - 2R$ for three different radii. In this and the following figures we have assumed a constant value of $u_0 = 0.30$ Ha.

In the asymptotic limit, $d \gg R_i$,

$$\frac{E_{\text{vdW}}}{L} = -\frac{9\pi^2}{64} \frac{J_{\text{tot}}(R_1, R_2, u_0^{(1)}, u_0^{(2)})}{d^5} \times$$

$$\times \left\{ 1 + \frac{25}{2} \frac{(R_1^2 + R_2^2)/2}{d^2} + \frac{3675}{32} \frac{(R_1^4 + 4R_1^2 R_2^2 + R_2^4)/6}{d^4} + \mathcal{O}\left(\frac{1}{d^6}\right) \right\} \quad (11)$$

we recover to lowest order the traditional London-theory macroscopic d^{-5} behavior [13] of two thin, parallel cylinders, albeit with different higher-order correction terms because nanotubes are hollow, not solid, cylinders. The limit of the expansion (11) is illustrated by the plots in Figure 3 for the identical tubes presented in Figure 2.

Figure 4 shows our results for another important special case, namely the concentric nanotube system [11]. When the two local nanotube coordinate systems coincide ($d = 0$) both of the two spatial integrals in (9) can be solved exactly [12, (2.584.58)] to give E_{vdW} in terms of the first and second complete Legendre elliptic integrals $K(k)$ and $E(k)$

$$\begin{aligned} \frac{E_{\text{vdW}}}{L} &= -\frac{3\pi}{32} \frac{J_{\text{tot}}(R_1, R_2, u_0^{(1)}, u_0^{(2)})}{(R_2 + R_1)^3 (R_2 - R_1)^2} \times \\ &\times \left\{ 4 \frac{R_2^2 + R_1^2}{(R_2 - R_1)^2} E\left(\frac{2\sqrt{R_1 R_2}}{R_1 + R_2}\right) - K\left(\frac{2\sqrt{R_1 R_2}}{R_1 + R_2}\right) \right\}. \end{aligned} \quad (12)$$

In Figure 4 the geometry part of (12), $E_{\text{vdW}}/(J_{\text{tot}}L)$, is shown.

We stress that the repulsive nanotube-nanotube interaction, resulting from the kinetic-energy repulsion, is not treated within our formalism.

IV. CONCLUSIONS

In summary, we report a quantum-physics calculation of the vdW binding in nanotube bundles and in concentric (multiwalled) nanotubes which is based directly on first-principle calculations of the electron density and on the electron density response. While present DFT implementations cannot account for the intertube interactions we have thus identified a method for a consistent combination with ab-initio calculations. Together with our recent progress for the layered systems our results indicate that a combined vdW-DF is feasible and hence promises an integration for a full quantum-physics account of the sparse and soft materials used for example in biophysics and nanotechnology.

V. ACKNOWLEDGMENTS

This work was supported by the Trygger Foundation, the Swedish Research Council (VR), and the Swedish Foundation for Strategic Research (SSF).

-
- [1] H. Rydberg, B. I. Lundqvist, D. C. Langreth and M. Dion, *Phys. Rev. B* **62**, 6997 (2000).
 - [2] B. I. Lundqvist et al., *Surface Sci.* **493**, 253 (2001).
 - [3] H. Rydberg, N. Jacobson, P. Hyldgaard, S. I. Simak, B. I. Lundqvist, and D. C. Langreth, *Surface Sci.* **532–535**, 606 (2003).
 - [4] H. Rydberg, M. Dion, N. Jacobson, E. Schröder, P. Hyldgaard, S. I. Simak, D. C. Langreth, and B. I. Lundqvist, *Van der Waals Density Functional for Layered Structures*, `cond-mat/0306033`.
 - [5] M.-F. Yu, B. S. Files, S. Arepalli, and R. S. Ruoff, *Phys. Rev. Lett.* **84**, 5552 (2000).
 - [6] J. Cumings and A. Zettl, *Science* **289**, 602 (2000).
 - [7] H. Dai, *Surf. Sci.* **500**, 218 (2001).
 - [8] L. A. Girifalco, M. Hodak, and R. S. Lee, *Phys. Rev. B* **62**, 13104 (2000).
 - [9] E. Schröder, *Phys. Rev. E* **62**, 8830 (2000).
 - [10] E. Hult, H. Rydberg, B. I. Lundqvist, and D. C. Langreth, *Phys. Rev. B* **59**, 4708 (1999).
 - [11] E. Schröder and P. Hyldgaard, *Surface Sci.* **532–535**, 880 (2003).
 - [12] I. S. Gradshteyn and I. M. Ryzhik, *Table of Integrals, Series, and Products*, 5th edition (Academic Press, San Diego, 1979).
 - [13] J. Mahanty and B. W. Ninham, *Dispersion Forces* (Academic Press, London, 1976).